CONFERENCE PRE-PRINT

SIMULATION OF FUEL INVENTORY IN DAMAGED TUNGSTEN UNDER SIMULTANEOUS HYDROGEN AND DEUTERIUM: SYNERGISTICAL EFFECT OF DEFECT ANNEALING AND ISOTOPE EXCHANGE

Zhenhou Wang

Key Laboratory of Materials Modification by Laser, Ion, and Electron Beams (Minister of Education), School of Physics, Dalian University of Technology

Dalian, People's Republic of China

Email: zhenhou@dlut.edu.cn

Chaofeng Sang

Key Laboratory of Materials Modification by Laser, Ion, and Electron Beams (Minister of Education), School of Physics, Dalian University of Technology

Dalian, People's Republic of China

Email: sang@dlut.edu.cn

Mengtao Li

Key Laboratory of Materials Modification by Laser, Ion, and Electron Beams (Minister of Education), School of Physics, Dalian University of Technology Dalian, People's Republic of China

Haiong Du Southwestern Institute of Physics Chengdu, People's Republic of China

Dezhen.Wang

Key Laboratory of Materials Modification by Laser, Ion, and Electron Beams (Minister of Education), School of Physics, Dalian University of Technology Dalian, People's Republic of China

Abstract

Tritium retention behavior in the first wall and divertor exhibits considerable complexity under multi-particle irradiation environments. Notably, neutron irradiation-induced damage substantially enhances tritium retention, presenting a significant challenge for accurately predicting the tritium inventory under simultaneous irradiation by multiple particle species. In this work, a model of coupling dynamic defect evolution with multiple hydrogen isotopes (HI) kinetics has been developed, to investigate fuel retention in tungsten (W) under simultaneous irradiation with high-energy W ions and HI (H and D). The simulations estimated the retention densities and distribution profiles of H and D in damaged W, revealing the underlying mechanisms of their interactions with induced traps. A strong competition between H and D for trapping sites was observed, indicating that D is preferentially trapped at vacancy-type defects than that of H, and their retention populations under simultaneous H and D irradiation with damage level (dpa) was evaluated. The synergistic effect of vacancy-type trap annealing and isotope exchange in reducing D retention. Furthermore, the effect of material temperatures and H/D flux ratios on D retention were discussed. The simulation results demonstrate that H/D exchange contributes to the reduction of D retention at low temperatures. As the temperature increases, defect annealing and thermal detrapping play increasingly important roles, which is beneficial to lower D inventory. It was found that increasing the H/D flux ratio decreases the trapped D concentration due to competitive exchange(H→D). The trapped D in W after simultaneous H and D irradiation was further reduced as continuous H implantation. In summary, this model integrates defect dynamics with isotopic exchange, offering predictive insights for controlling HI inventory in plasma-facing materials (PFMs) of fusion reactors.

1. INTRODUCTION

The management of tritium (T) inventory in plasma-facing materials (PFMs) for future fusion reactors is a critical concern due to radiological safety risks associated with tritium retention [1]. Consequently, stringent control of T accumulation in PFMs is imperative. Tungsten (W) has emerged as the primary candidate for PFMs owing to its favourable properties, including low intrinsic T retention. However, during tokamak operation, PFMs are subjected to simultaneous bombardment by hydrogen isotope (HI) ions (D, T) and high-energy neutrons, leading to the formation of lattice defects that exacerbate T retention. Notably, 14 MeV neutron irradiation generates dense populations of defects with high trapping energies (e.g., vacancy clusters, voids), which dominate T

inventory build-up in DT fusion scenarios [2]. Extensive research has focused on predicting HI retention in neutron-damaged PFMs. A significant limitation persists: direct experimental studies of neutron-induced damage remain scarce, necessitating the use of ion irradiation as a proxy[3][4]. Recent experimental and computational advances have elucidated key mechanisms, demonstrating that trapping and de-trapping kinetics at radiation induced defects govern fuel retention[5][6]. Nevertheless, prevailing studies exhibit two critical shortcomings. On one hand, most retention data derive from single-species HI irradiation, neglecting synergistic effects of mixed H/D/T fluxes characteristic of reactor plasmas. The isotopic effects on HI retention under multi-species HI irradiation is interesting, e.g., isotope exchange effect. On the other hand, defect evolution dynamics (e.g., recombination, clustering) under prolonged irradiation are rarely incorporated in multiple-species irradiation, despite their profound influence on trap site populations. The evolution of defects in PFMs is a stochastic, nonlinear process governed by competing mechanisms such as defect annealing and HI trapping-detrapping kinetics. Experimental study of this dynamic evolution remains prohibitively challenging, consequently, advanced multiscale numerical modelling becomes indispensable to unravel defect-HI synergies and predict T inventory in PFMs under reactor-relevant conditions.

Research on HI retention has predominantly examined sequential irradiation schemes involving H, D, and T, yielding preliminary understanding of their distinct retention behavior and mutual interactions [7–10]. Experimental studies showed that H implantation in self-damaged tungsten effectively reduces D retention. Computationally, recent modelling efforts have estimated D-T retention in co-deposited layers[11], while Sun et al. investigated HI retention and exchange under sequential H-D irradiation[12], confirming the isotope exchange for removal D. Nevertheless, existing studies consistently overlook the dynamic evolution of irradiation-induced defects and lack mechanistic analysis under simultaneous multi-particle irradiation. To systematically simulate multiple HI behavior in W, we simulated the D retention in W under the irradiation with W ions, H and D plasmas, with particular emphasis on the coupling between defect evolution and isotope exchange mechanisms.

In our previous work [13], we developed a Hydrogen Isotope Inventory Process Code (HIIPC) to assess fuel retention in self-ion damaged W under sequential D and H irradiation, and found that the trapped D is reduced during H irradiation due to the occurrence of the isotope exchange (H \rightarrow D). However, our preliminary results demonstrated that the reduce D retention by isotopic exchange is limited due to static defect assumption and oversimplified exchange. To address these gaps, our recent work [14] established a dynamic defect VITDE model that quantifies vacancy/interstitial-type defect evolution populations under simultaneous W-ion bombardment and thermal annealing, providing time-resolved trap site densities for HI retention.

In the present work, building upon our previous works [13][14][15], a coupled VITDE-HIIPC model that incorporates multi-species HI bombardment and defect dynamics is developed and is used to simulate H and D retention in radiation-damaged W under simultaneous H/D irradiation. The primary objective is to elucidate the synergistic interplay between defect annealing kinetics and isotopic exchange mechanisms in governing HI retention, and estimate the H and D concentration and distributions inside W.

SIMULATION MODEL

The VITDE-HIIPC model describes the co-evolution of three key field quantities under multi-species particle bombardment: the concentrations of irradiation-induced interstitial-type defect clusters (In), vacancy-type defect clusters (V_n), and hydrogen isotopes (H and D). Within a continuum framework, their temporal and spatial development is governed by the following set of coupled differential equations:

$$\frac{\partial c_{I_{n}}(z,t)}{\partial t} = G_{I_{n}} + D_{I_{n}}(T) \frac{\partial^{2} c_{I_{n}}}{\partial z^{2}} - \frac{\partial c_{I_{n}-I_{m}}^{clust}}{\partial t} - \frac{\partial c_{V_{n}-I_{m}}^{recom}}{\partial t} - \frac{\partial c_{I_{n}}^{D}}{\partial t} - \sum_{i=1}^{M} \frac{\partial c_{sink,i}^{I_{n}}}{\partial t} \\ \frac{\partial c_{V_{n}}(z,t)}{\partial t} = G_{V_{n}} + D_{V_{n}}(T) \frac{\partial^{2} c_{V_{n}}}{\partial z^{2}} - \frac{\partial c_{V_{n}-V_{m}}^{clust}}{\partial t} - \frac{\partial c_{V_{n}-I_{m}}^{recom}}{\partial t} - \frac{\partial c_{V_{n}}^{D}}{\partial t} - \frac{\partial c_{V_{n}}^{V_{n}}}{\partial t} - \sum_{i=1}^{M} \frac{\partial c_{sink,i}^{V_{n}}}{\partial t}$$

$$(1)$$

$$\frac{\partial C_{V_n}(z,t)}{\partial t} = G_{V_n} + D_{V_n}(T) \frac{\partial^2 C_{V_n}}{\partial z^2} - \frac{\partial C_{V_n-V_m}^{lett,n}}{\partial t} - \frac{\partial C_{V_n-V_m}^{lett,n}}{\partial t} - \frac{\partial C_{V_n}^{lett,n}}{\partial t} - \frac{\partial C_{V_n}^{lett,n}}{\partial t} - \sum_{i=1}^{M} \frac{\partial C_{sink,i}^{lett,n}}{\partial t}$$
(2)

$$\frac{\partial \mathcal{C}_{S}^{D}(z,t)}{\partial t} = G_{D} + D_{D}(T) \frac{\partial^{2} \mathcal{C}_{S}^{D}}{\partial z^{2}} - \sum_{i=1}^{M} \frac{\partial \mathcal{C}_{Sink,i}^{D}}{\partial t} - \sum_{n=1}^{N} \frac{\partial \mathcal{C}_{V_{n}}^{D}}{\partial t}$$

$$\tag{3}$$

$$\frac{\partial c_s^H(z,t)}{\partial t} = G_H + D_H(T) \frac{\partial^2 c_s^H}{\partial z^2} - \sum_{i=1}^M \frac{\partial c_{sink,i}^H}{\partial t} - \sum_{n=1}^N \frac{\partial c_{v_n}^H}{\partial t}$$
(4)

$$\frac{\partial C_{V_n}^{D}}{\partial t} = \omega_{D,V_n}^{+} C_s^{D} C_{V_n} - \omega_{D+V_n}^{-} C_{V_n}^{D} exp\left(-\frac{E_{V_n-D}^{dt}}{k_h T}\right) - v_0 e^{-\frac{E_{Swap}}{k_b T}} \left(\frac{C_s^{H} C_t^{D} - C_s^{D} C_t^{H}}{N_T}\right)$$
 (5)

$$\frac{\partial C_{V_n}^H}{\partial t} = \omega_{D,V_n}^+ C_s^H C_{V_n} - \omega_{D+V_n}^- C_{V_n}^H exp\left(-\frac{E_{V_n-H}^{dt}}{k_h T}\right) - v_0 e^{-\frac{E_{Swap}}{k_h T}} \left(\frac{C_s^D C_t^H - C_s^H C_t^D}{N_T}\right)$$
(6)

In this model, the production rates of interstitial-type (I_n) and vacancy-type (V_n) defect clusters, as well as the implantation profiles of H/D, are determined using theoretical formulations and TRIM simulations. The resulting defects interact with implanted H/D through a series of key processes—including diffusion, reaction, clustering, dissociation, trapping, and de-trapping—whose rates are governed by physical parameters such as diffusion coefficients, capture radii, defect-defect binding energies, and H/D trapping/de-trapping energies. Key irradiation conditions, including H/D particle fluxes, damage rates induced by W ions, and material temperature, are explicitly incorporated into the model.

TABLE 1. The de-trapping parameters of all the trap sites for HI used in simulation

Trap types	Symbols	Values
GB	$E^{dt}_{GB-D}(eV)$	0.85
Dis	$E_{Dis-D}^{dt}(eV)$	1.0
$V_n(n=1\sim N=10)$	$E_{V_n-D}^{dt}(\mathrm{eV})$	1.42,1.56,1.60,1.65,1.69,
		1.71,1.75,1.79,1.82,1.85

3. SIMULATION RESULTS

The creation and evolution of defects under hydrogen isotope (HI) irradiation play a critical role in fuel retention. We simulated the retention of H and D in W under simultaneous H/D irradiation coupled with W-ion damage. The D particle flux $I_D = 1.1 \times 10^{18} \, \text{m}^{-2} \text{s}^{-1}$ and H particle flux is equal to λI_D , here λ is denoted as H and D flux ratio (λ =2 is fixed unless otherwise stated). Fig. 1 presents the trapped H and D concentration profiles in the damaged region at 300 K. The W-ion damage rate of $2 \times 10^{-4} \text{dpa/s}$ is used, and irradiation time is set to 1h. For reference, the D concentration profile under mono-species D irradiation is also calculated and plotted. The higher retained H concentration compared to D is ascribed to its larger trapping rate in vacancy-type defects. Furthermore, under simultaneous irradiation, D exhibits a greater retention depth than in the mono-species case, indicating that the H-D competition for traps enhances the diffusion and transport of both isotopes into the bulk.

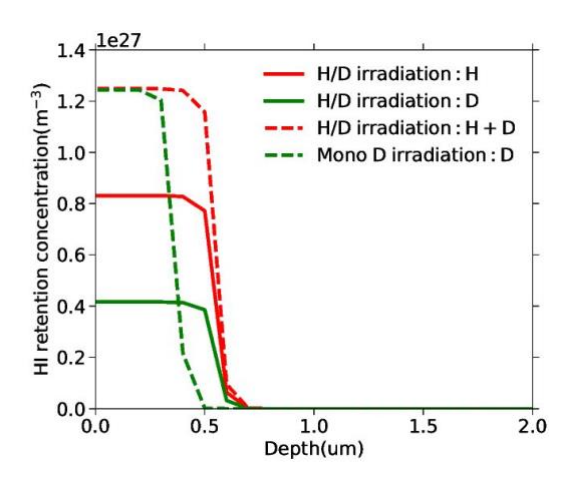


Fig. 1. Distributions of retained H and D concentrations in W under simultaneous 20MeV W ions and 200eV HI particles at 300K. The damage rate of 2×10^{-4} dpa/s is used and irradiation time 1h.

We further investigated the influence of varying damage levels (dpa) on the retention and transport of H and D under simultaneous H/D irradiation and W-ion damage. Fig.2 shows the evolution of trapped H (C_{Vn}^H , Fig. 2(a)) and trapped D (C_{Vn}^D , Fig. 2(b)), and the concentration of created vacancy-type traps a function of dpa after 1 hour of simultaneous irradiation at 300K. As the dpa increases from 0.07 to 1.0, the maximum values of C_{Vn}^H , C_{Vn}^D and $C_{Vn}^{created}$ all rise, while their penetration depths decrease. A higher damage rate accelerates the filling of the generated V_n , thereby slowing the diffusion of hydrogen isotopes. Moreover, as shown in

Fig. 2(c), the concentration of created V_n traps increases significantly within the H and D retention region (<1.1 µm), compared to regions not occupied by H or D. Additionally, simulations at an elevated temperature of 600 K illustrate the evolution of $C_{V_n}^H$, $C_{V_n}^D$ and $C_{V_n}^{created}$ with dpa, as shown in Fig. 3. The results indicate that all three concentrations within the damaged region (~2.3 µm) saturate at damage levels below 0.54 dpa. A comparison of Figs. 3(a-c) reveals that the trapped deuterium ($C_{V_n}^D$) accounts for the majority of the total created $C_{V_n}^{created}$.

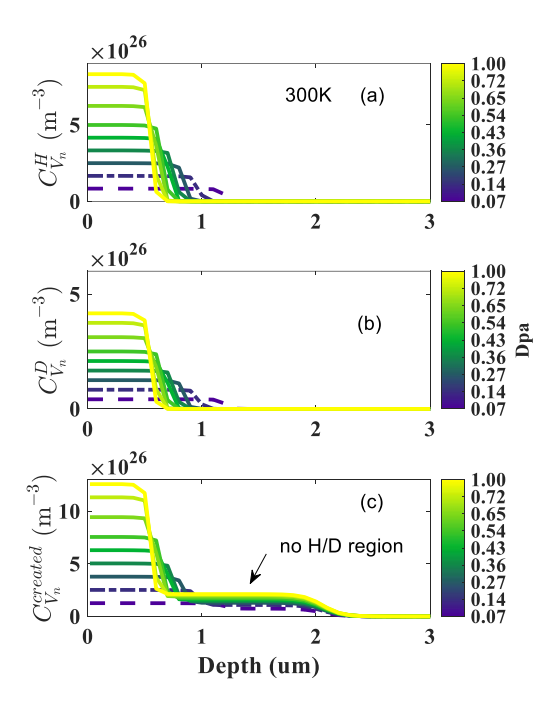


Fig. 2. Variations of H, D and induced traps concentrations as dpa raises in W after simultaneous high energy W ions and low energy HI particles at 300K. The irradiation time is fixed as 1h.

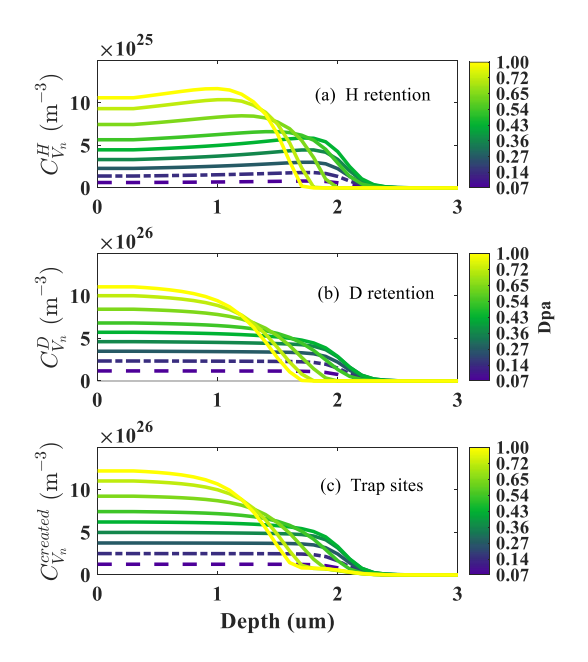


Fig. 3. Variations of H, D and induced traps concentrations with dpa in W after simultaneous high energy W ions and low energy HI particles at 600K.

In fusion reactors, the first wall and divertor are subjected to direct bombardment by D and T particles, whose flux ratio may vary. This present study aims to elucidate the distribution of H and D and their influence on defect production under H/D co-irradiation with varying flux ratios. Fig. 4 presents the evolution of $C_{V_n}^H$, $C_{V_n}^D$ and $C_{V_n}^{created}$ as a function of the H/D flux ratio during simultaneous irradiation at 300 K, under a W-ion damage rate of 2×10^{-4} dpa/s for 1 hour. As the H/D flux ratio increases, the maximum concentration of $C_{V_n}^H$ rises (Fig. 4(a)), while that of $C_{V_n}^D$ declines (Fig. 4(b)). This trend is attributed to the increased solute H concentration at higher H fluxes, which enhances the filling rate of available trapping sites. As a result, H exhibits a stronger trapping affinity than D, leading to preferential occupation of defect sites by H and a consequent suppression of D trapping. Furthermore, with increasing H/D flux ratio, the retention depths of both $C_{V_n}^H$ and $C_{V_n}^D$ increase. The dominant trapping of solute H reduces the effective trapping of solute D, thereby promoting its deeper diffusion into the material. In additional, the observed reduction in trapped D concentration under elevated H flux further indicates significant H-D isotope exchange at 300 K. Fig. 4(c) shows the variation of $C_{V_n}^{created}$ with the H/D flux ratio. While the depth of the created vacancy-type traps profile increases, its maximum concentration remains largely unchanged.

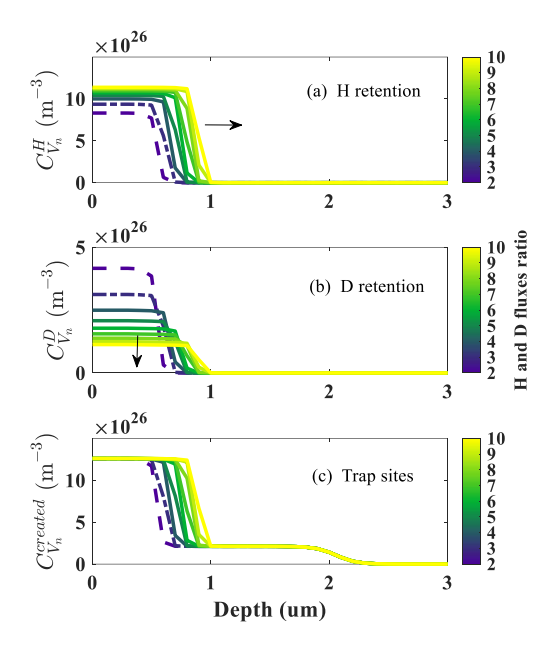


Fig. 4. Variations of H, D and induced traps concentrations with H and D flux ratio in W after simultaneous high energy W ions and low energy HI particles at 300K.

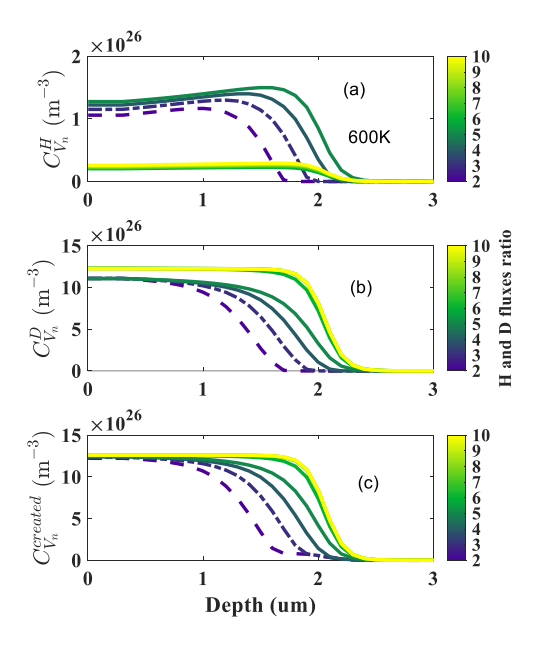


Fig.5. Variations of H, D and induced traps concentrations with H and D flux ratios in W after simultaneous high energy W ions and low energy HI particles at 600K.

A strong interdependence is observed between the H/D flux ratio, material temperature, and their combined effect on hydrogen isotope retention and defect formation. The simulated values of $C_{V_n}^H$, $C_{V_n}^D$ and $C_{V_n}^{created}$ at 600 K are shown in Fig. 5 as a function of the H/D flux ratio. The trends for $C_{V_n}^H$ and $C_{V_n}^D$ at this temperature differ from those in Fig. 4(a, b), revealing a mechanistic shift. The data in Fig. 5 indicate that $C_{V_n}^H$ first rises then falls, while $C_{V_n}^D$ increases monotonically until both saturate. The total concentration of created vacancy clusters $C_{V_n}^{created}$ in the damaged region also reaches saturation with an increasing H/D flux ratio.

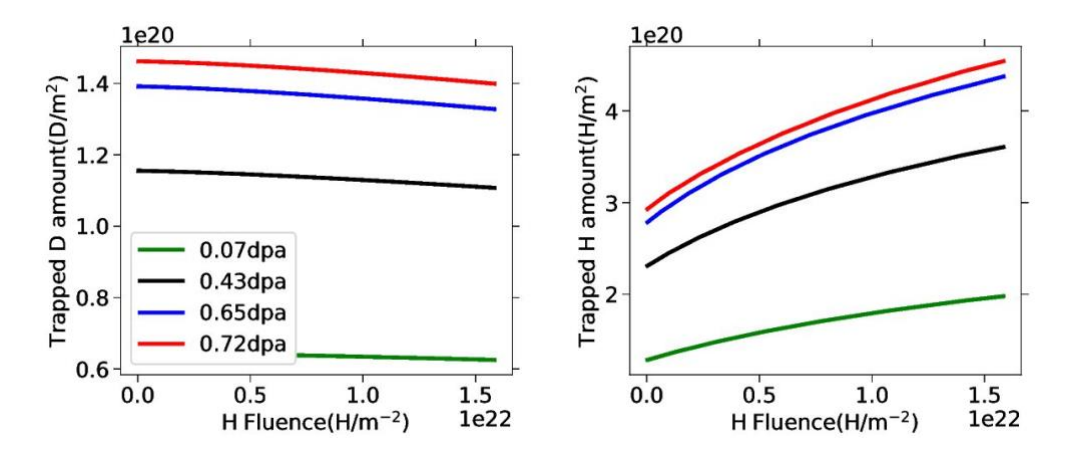


Fig.6. Variations of H, D and induced traps concentrations with H and D flux ratio in W after simultaneous high energy W ions and low energy HI particles at 300K.

To elucidate the isotope exchange of trapped D within an evolving defect system, the simultaneous damaged W containing trapped H and D was subjected to subsequent hydrogen (H) irradiation. Fig. 6 depicts the evolution of the areal densities of trapped H and D at different damage levels (dpa) during continuous H irradiation at 300 K, following the cessation of the D flux. As shown in Fig. 6(a), the trapped D concentration decreases with increasing H fluence, which is accompanied by a concurrent rise in trapped H. This reduction in D is attributed to the isotopic replacement of trapped D by incoming H atoms.

4. CONCLUSIONS AND DISCUSSIONS

In the present work, fuel retention behavior under simultaneous irradiation with tungsten ions and hydrogen/deuterium (H/D) is investigated. The retention mechanisms of H/D and their interactions with irradiation-induced defects are analyzed by taking into account defect annealing and hydrogen isotope exchange. Simulations reveal the density and spatial distribution of retained hydrogen and deuterium. The results demonstrate that under H/D co-irradiation, the isotope retention depth increases significantly compared to single-species deuterium irradiation. The retention density of both hydrogen and deuterium rises with increasing radiation damage, as higher damage rates promote defect generation and enhance trapping, thereby suppressing H/D diffusion and reducing the retention depth. The trapped H/D density shows a strong dependence on material temperature and the H/D flux ratio. At lower temperatures, hydrogen retention exceeds that of deuterium, whereas this trend reverses at elevated temperatures. Increasing the H/D flux ratio at low temperatures effectively reduces trapped deuterium, and further deuterium removal can be achieved through hydrogen isotope exchange during continued hydrogen irradiation. These simulation results provide an insight for predicting and mitigating fuel retention under deuterium-tritium irradiation in future fusion reactors.

ACKNOWLEDGEMENTS

This work is supported by National Key R&D Program of China No. 2022YFE03180300, LiaoNing Province Science and Technology Project 2024JH2/102600021, and DUTZD25113.

REFERENCES

- [1] Roth J, Tsitrone E, Loarer T, Philipps V, Brezinsek S, Loarte A, Counsell G F, Doerner R P, Schmid K, Ogorodnikova O V and Causey R a 2008 Tritium inventory in ITER plasma-facing materials and tritium removal procedures *Plasma Phys. Control. Fusion* **50** 103001
- [2] Shimada M, Cao G, Otsuka T, Hara M, Kobayashi M, Oya Y and Hatano Y 2015 Irradiation effect on deuterium behaviour in low-dose HFIR neutron-irradiated tungsten *Nucl. Fusion* **55** 013008
- [3] Wampler W R and Doerner R P 2009 The influence of displacement damage on deuterium retention in tungsten exposed to plasma *Nucl. Fusion* **49** 115023
- [4] Hoen M H J 't, Tyburska-Püschel B, Ertl K, Mayer M, Rapp J, Kleyn A W and Zeijlmans van Emmichoven P A 2012 Saturation of deuterium retention in self-damaged tungsten exposed to high-flux plasmas *Nucl. Fusion* **52** 023008
- [5] Založnik A, Markelj S, Schwarz-Selinger T and Schmid K 2017 Deuterium atom loading of self-damaged tungsten at different sample temperatures *J. Nucl. Mater.* **496** 1–8
- [6] Barton J L, Wang Y Q, Doerner R P and Tynan G R 2016 Model development of plasma implanted hydrogenic diffusion and trapping in ion beam damaged tungsten *Nucl. Fusion* **56** 106030
- [7] Ogorodnikova O V, Markelj S, Efimov V S and Gasparyan Y M 2016 Deuterium removal from radiation damage in tungsten by isotopic exchange with hydrogen atomic beam *J. Phys. Conf. Ser.* **748** 012007
- [8] Markelj S, Založnik A, Schwarz-Selinger T, Ogorodnikova O V, Vavpetič P, Pelicon P and Čadež I 2016 In situ NRA study of hydrogen isotope exchange in self-ion damaged tungsten exposed to neutral atoms *J. Nucl. Mater.* **469** 133–44
- [9] Matveev D, Hansen P, Dittmar T, Koslowski H R and Linsmeier C 2019 Modeling of H/D isotope-exchange in crystalline beryllium *Nucl. Mater. Energy* **20** 100682
- [10] Barton J L, Wang Y Q, Doerner R P and Tynan G R 2015 Development of an analytical diffusion model for modeling hydrogen isotope exchange *J. Nucl. Mater.* **463** 1129–33
- [11] Krat S, Prishvitsyn A and Gasparyan Y 2024 Theoretical estimation of multiple hydrogen isotope content in metal layers slowly co-deposited from plasmas *J. Nucl. Mater.* **588** 154793
- [12] Sun F, Hao C, Chen D Y, Zhou H S, Oya Y, Zhu J P, Tang J, Zong H, Luo L M and Wu Y C 2024 Mechanism of hydrogen isotope exchange for tritium removal in plasma-facing materials: a multi-scale investigation *Nucl. Fusion* **64** 046011
- [13] Wang Z, Sang C, Chang M, Liu S and Wang D 2018 Modeling of fuel retention and hydrogen-isotope exchange removal from the pre-damaged tungsten material *Fusion Eng. Des.* **136** 372–6
- [14] Wang Z, Sang C and Wang D 2024 Simulation of defect evolution in tungsten during annealing by developing a vacancy and interstitial-type defect evolution model *Phys. Scr.* **99** 025617
- [15] Wang Z, Sang C and Wang D 2020 Modelling of deuterium retention and outgassing in self-damaged tungsten under low-energy atomic D flux irradiation: The effects of surface processes *J. Nucl. Mater.* **540** 152390